Inorganic Chemistry

Article

pubs.acs.org/IC

Microwave-Assisted Solvothermal Synthesis of Spinel AV_2O_4 (M = Mg, Mn, Fe, and Co)

Arturo Gutierrez and Arumugam Manthiram*

Materials Science and Engineering Program and Texas Materials Institute, The University of Texas at Austin, 1 University Station C2200, Austin, Texas 78712, United States

Supporting Information

ABSTRACT: Lower-valent vanadium oxide spinels AV_2O_4 (A = Mg, Mn, Fe, and Co) consisting of A^{2+} and V^{3+} ions have been synthesized by a low-temperature microwave-assisted solvothermal (MW-ST) synthesis process in a tetraethylene glycol (TEG) medium. The oxides are formed within a short reaction time of 30 min at 300 °C. Subsequent postheat treatment of the oxides at elevated temperatures in inert or reducing atmospheres results in an instability of the spinel phase, especially CoV_2O_4 due to the ease of formation of metallic Co, demonstrating the advantage of the low-temperature MW-ST process in accessing these oxides. This MW-ST synthesis approach is attractive for synthesizing other lower-valent transition-metal oxides that are otherwise difficult to obtain by conventional synthesis methods and for subsequent study of their unique physical and chemical properties.

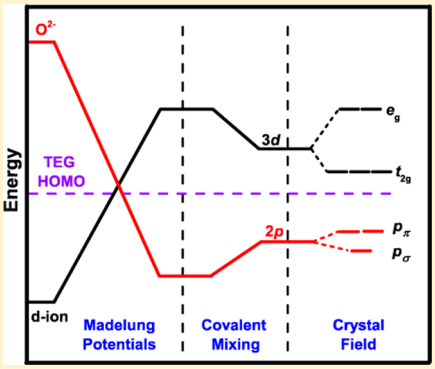

INTRODUCTION

The AV_2O_4 spinel oxides consisting of A^{2+} and V^{3+} ions exhibit interesting electrical and magnetic properties.[1] Particularly, the electronic properties of the AV_2O_4 spinel oxides undergo a transition from localized to itinerant-electron behavior when they undergo a first-order quantum phase transition (QPT). An approach of the QPT can occur from either the itinerant or localized-electron side. Of particular interest to solid state physicist and chemists when approaching the QPT from the localized limit is the possibility of tuning the ratio between the electronic hopping and intra-atomic Coulomb energy U by changing the size of the A^{2+} ions in AV_2O_4.[1,2] However, experimental evidence[3] and theoretical calculations[4] suggest that a charge gap opens due to strong correlations before the itinerant electron behavior occurs. In this regard, the synthesis and stabilization of AV_2O_4 oxides with various A^{2+} ions having different sizes could help to develop a better fundamental understanding of the physical phenomena occurring as a function of V−V distance.

However, the synthesis of oxides containing lower-valent V^{3+} ions requires reactions of the component oxides in a reducing or inert gas atmosphere (e.g., H_2, Ar−H_2 mixture, N_2−H_2 mixture, Ar, or N_2) or sealed tubes under vacuum at elevated temperatures (≥800 °C). These reactions often require prolonged reaction times (e.g., several hours to days) at high temperatures with repeated intermittent grindings, as V_2O_3 is refractory with a high melting temperature.[5−8] Unfortunately, ions like Co^{2+} can get easily reduced to the metallic state (e.g., Co metal) at those elevated temperatures, resulting in an inaccessibility of the spinel phase.

Interestingly microwave-assisted solvothermal (MW-ST) reactions in a suitable solvent can offer desired products at relatively lower temperatures within a short reaction time (e.g., within minutes).[9−19] Due to the much lower reaction temperatures involved, the MW-ST processes can also provide access to metastable phases that are otherwise inaccessible by high-temperature processes, as has been, for example, shown recently by the facile reduction of transition-metal oxides with tetraethylene glycol (TEG) as a reducing agent.[20]

We present here a rapid MW-ST process in TEG medium employing precursor solutions for synthesizing the AV_2O_4 (Mg, Mn, Fe, and Co) spinel oxides within a short time of 30 min at a low temperature of 300 °C. The method exploits the reducing strength of TEG and the low energy levels of the cations in solution before the formation of the AV_2O_4 crystals. Subsequent postheat treatment of the AV_2O_4 samples in an inert or reducing atmosphere at elevated temperatures demonstrates the advantage of the low-temperature MW-ST method as oxides like CoV_2O_4 gets reduced to give Co metal at high temperatures.

EXPERIMENTAL SECTION

AV_2O_4 (M = Mg, Fe, Mn, and Co) samples were prepared by first mixing vanadium triisopropoxide oxide (Alfa Aesar, 96%) with the appropriate divalent metal acetate tetrahydrate (Mg, Fe, Mn, or Co) in TEG (Alfa Aesar) and stirring continuously for several hours to allow the precursors to dissolve. The solution was then placed in an Anton-Paar Monowave 300 microwave synthesis reactor, where it was heated as fast as possible to 300 °C (generally reached in 2 min). The mixture was stirred during the reaction at 800 rpm with a magnetic stir bar and held at the maximum temperature of 300 °C for 30 min while being monitored by an infrared temperature sensor. The pressure inside of

Received: May 20, 2014
Published: August 6, 2014

   dx.doi.org/10.1021/ic5011506 | Inorg. Chem. 2014, 53, 8570−8576

the vessels generally stayed between 15 and 25 bar. After the cooling cycle was completed, the products were sonicated, centrifuged, and washed with acetone until the decanted solution was clear. The samples were then dried in air overnight before postheating to temperatures between 450 and 900 °C in a flowing 5% H_2−95% Ar or 100% Ar atmosphere. The length of time for the postheating treatment varied between 3 and 48 h.

The chemical compositional analysis was carried out by inductively coupled plasma (ICP) analysis with a Varian 715-ES ICP optical emission spectrometer. X-ray powder diffraction (XRD) data were collected with a Rigaku Ultima IV instrument with Cu Kα radiation. Scanning electron microscopy[21] images and elemental dot maps were carried out with a Hitachi S5500 SEM/STEM microscope with energy dispersive spectroscopic (EDS) capability.

RESULTS AND DISCUSSION

Conventional heating is a slow and inefficient method for transferring energy to a reaction mixture because it depends on convective heating and on the thermal conductivity of the precursors and products involved in the reaction. On the other hand, microwave-assisted synthesis is efficient at uniformly heating the whole liquid volume through two main mechanisms: dipolar polarization and ionic conduction.[22] The molecular dipoles in the solvent realign themselves with the oscillating electric field and lose energy in the form of heat through molecular friction and dielectric loss. In a similar fashion, under the influence of an oscillating electric field, charged particles collide with atoms and molecules in the solution and generate heat.

The loss tangent (tan δ) of a material or solvent quantifies its ability to convert microwave energy into heat. A solvent with a high loss tangent value is required for efficient heating, but solvents with moderate to low microwave absorptivity can also be used for synthesis. When one chooses a solvent for microwave synthesis, other relevant properties must also be considered. Several solvents were investigated in the synthesis of AV_2O_4 (Mg, Mn, Fe, and Co) to demonstrate this: deionized (DI) water, polyethylene glycol (PEG), and TEG. Although the hydrothermal process is the most commonly used method to generate oxides in solvent-based reactions,[22] the use of deionized water as the solvent resulted in a mixture of cobalt and vanadium oxide phases (e.g., V_6O_{13} and Co_3O_4). The mixed cobalt and vanadium oxides that formed were higher valent oxides of vanadium as indicated by the above formulas, suggesting that water is not a strong enough reducing agent under these conditions to obtain the desired V^{3+} oxides. In addition, the maximum temperature achieved when using DI water was 240 °C, which may have played a role in the inability to successfully form AV_2O_4. Polyethylene glycol (PEG) has also been used to assist in the formation of transition-metal oxides in microwave-assisted processes.[23,24] Even though a higher reaction temperature was achieved (300 °C) when using PEG as the solvent, the solid that formed during the reaction was amorphous.

The higher boiling point (>300 °C) and reducing strength of TEG combined to facilitate the formation of the lower-valent vanadium spinel oxides AV_2O_4. Figure 1a shows the XRD patterns of AV_2O_4 (A = Mg, Mn, Fe, and Co) synthesized in TEG at 300 °C for 30 min. The broad peaks are a result of the small crystallite size (Figure 1b). The samples formed secondary particles in the range 75−100 nm made up of primary particles between 5 and 10 nm in diameter. With the exception of the FeV_2O_4 sample, all peaks in the samples could be indexed to $Fd\bar{3}m$. The XRD pattern of the intended FeV_2O_4 sample showed impurity peaks in addition to the peaks for FeV_2O_4. The actual impurity is hard to identify due to the low crystallinity of the pattern, but Fe_2O_3 (space group $R\bar{3}c$) is a possibility. We mapped several particles in each of the samples and found the distribution of the elements to be homogeneous (Figure 1c). The ICP analysis (Supporting Information Table S1) indicated the elemental ratios in each of the samples were near the expected values.

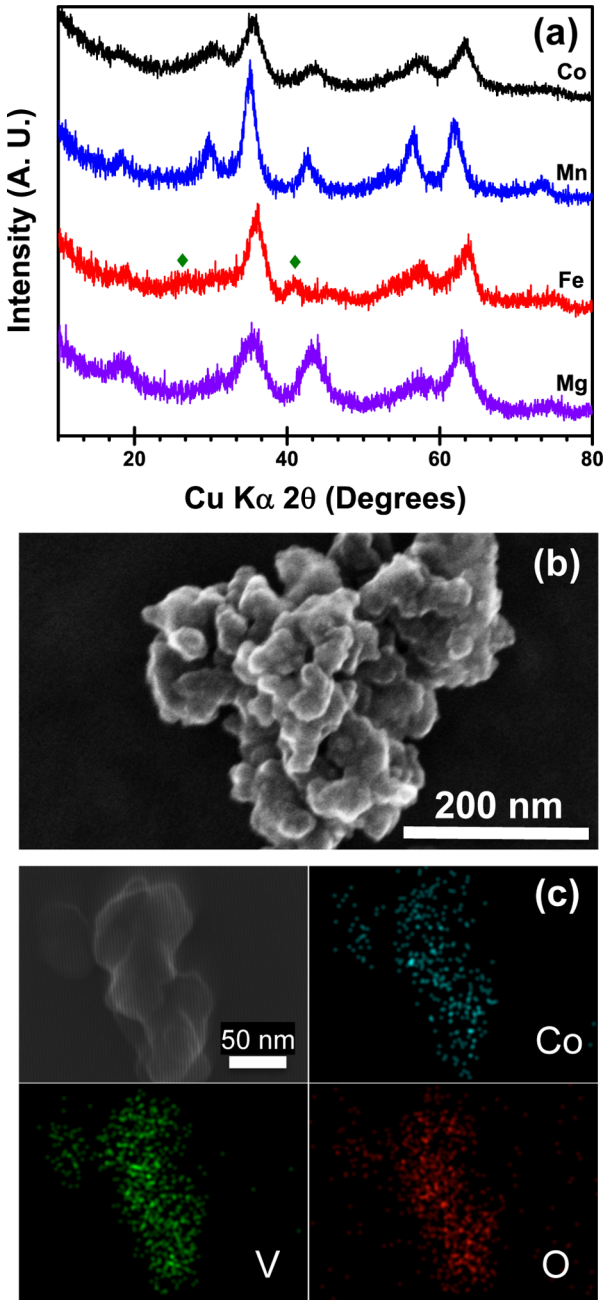

Figure 1. (a) XRD patterns of AV_2O_4 (A = Mg, Mn, Fe, and Co) synthesized by the MW-ST method at 300 °C for 30 min in TEG solvent; the green diamond indicates impurity peaks, possibly due to Fe_2O_3 (space group $R\bar{3}c$). (b) SEM image representing the morphology of each of the AV_2O_4 samples synthesized by the MW-ST method at 300 °C for 30 min in TEG with a Monowave 300 microwave reactor system. (c) EDS mapping of elements on CoV_2O_4, showing a homogeneous distribution.

dx.doi.org/10.1021/ic5011506 | Inorg. Chem. 2014, 53, 8570−8576

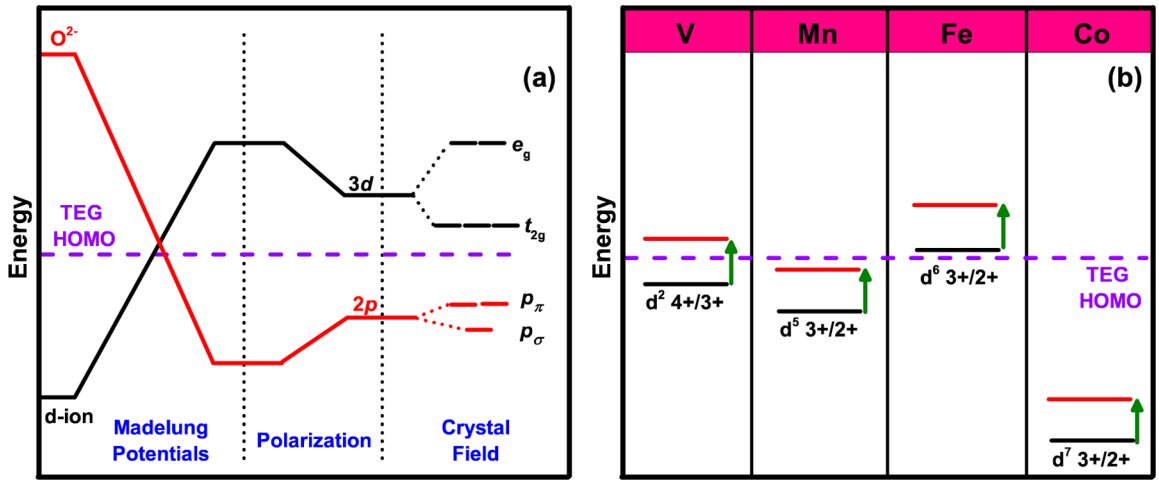

Figure 2. (a) Qualitative energy diagram summarizing the parameters that influence the M:3d and O:2p energy levels, with the energy levels of the ions in solution shown on the left of the diagram. (b) Energy diagram depicting the location of the cation energy levels in reference to the HOMO in TEG in solution (black line) and after the crystalline solid is formed (red line).

Our group has demonstrated previously that the ability to reduce transition-metal oxide (solid) suspensions in a solvent through a microwave-assisted method is dependent on the location of the highest occupied molecular orbital (HOMO) of the solvent in reference to the energy of the redox couple in the oxide.[20] The current work exploits the energy of the cations in solution, which is lower than that in solids, before they combine to form AV_2O_4. Figure 2a provides a schematic of how the energy levels shift due to larger electrostatic potentials (Madelung energy) that arise when ions are brought together to form the crystal solid. The Madelung potential is approximated by treating the ions in the lattice as point charges. The negative charge on the oxide ions produces a *repulsive* Madelung potential at the cation sites, which decreases the effective ionization energy (raises the energy level) of the electrons in the cation. The positive charge on the cations provides an *attractive* Madelung potential at the oxygen site, which lowers the energy level of the oxygen below that of the cations. The effect of polarization brings the energy levels closer together as shown. When the crystal is formed, the oxide ions surrounding the cations constitute a crystal field around the cations and spilt the d-orbitals into t_{2g} and e_g levels. The oxide ions experience an axial crystal field, and the p-orbitals of oxygen are classified as either sigma (p_σ) or pi (p_π) bonding.

Figure 2b depicts the energy levels of the cations in solution and in the solid with respect to the HOMO in TEG. The $V^{3+/4+}$ and $Mn^{2+/3+}$ couples are similar in energy as evidenced by our recent work in vanadium-doped phosphate cathode materials, where the redox potentials of $V^{3+/4+}$ and $Mn^{2+/3+}$ were shown to be the same (~4.1 vs Li/Li^+).[25] As described above, the energy level for $V^{3+/4+}$ in solution is slightly lower than the HOMO in TEG, which allows access to V^{3+} and the formation of AV_2O_4. After the crystal structure forms, the $V^{3+/4+}$ energy level shifts above the HOMO in TEG making the 3+/4+ couple inaccessible in the solid as has been shown previously by our group.[20] The $Mn^{2+/3+}$ and $Co^{2+/3+}$ energy levels lie below the HOMO in TEG for both the solid and solution as both redox couples are accessible in the solid[20] and in solution (this work). Even with the shift to a lower energy in solution, the $Fe^{2+/3+}$ couple is above the HOMO, making it inaccessible as evidenced by the difficulty in obtaining the pure FeV_2O_4 phase directly from the MW-ST synthesis as it also contained an impurity phase (possibly Fe_2O_3).

We attempted to improve the crystallinity of the samples obtained by the MW-ST process by increasing the hold time for the MW-ST reaction. Due to the safety limits inherent to the Monowave 300 reactor system, longer dwell times (>30 min) at 300 °C are not possible. Therefore, the experiments for testing the effect of dwell time of the reaction were carried out in a Synthos 3000 microwave reactor. A preliminary run was carried out to ensure that comparable results would occur in each of the reactors. The similar XRD patterns and morphology (Figures S1 and S2b in the Supporting Information) for CoV_2O_4 synthesized at 300 °C for 30 min in the Synthos and Monowave systems suggest that any differences are negligible.

The AV_2O_4 samples were synthesized in the Synthos at 300 °C with a hold time of 30 min, 2 h, and 4 h. As seen in Figure 3, the XRD peaks for the samples are sharper and more easily resolved as the dwell time increases. The size of the secondary particles for the material also grew with increasing dwell time.

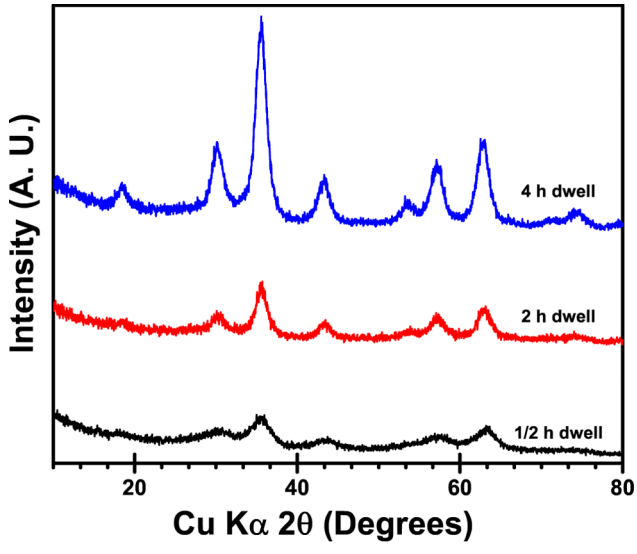

Figure 3. XRD patterns of CoV_2O_4 synthesized in the Synthos 3000 microwave reactor system at 300 °C and held for different dwell times.

dx.doi.org/10.1021/ic5011506 | Inorg. Chem. 2014, 53, 8570−8576

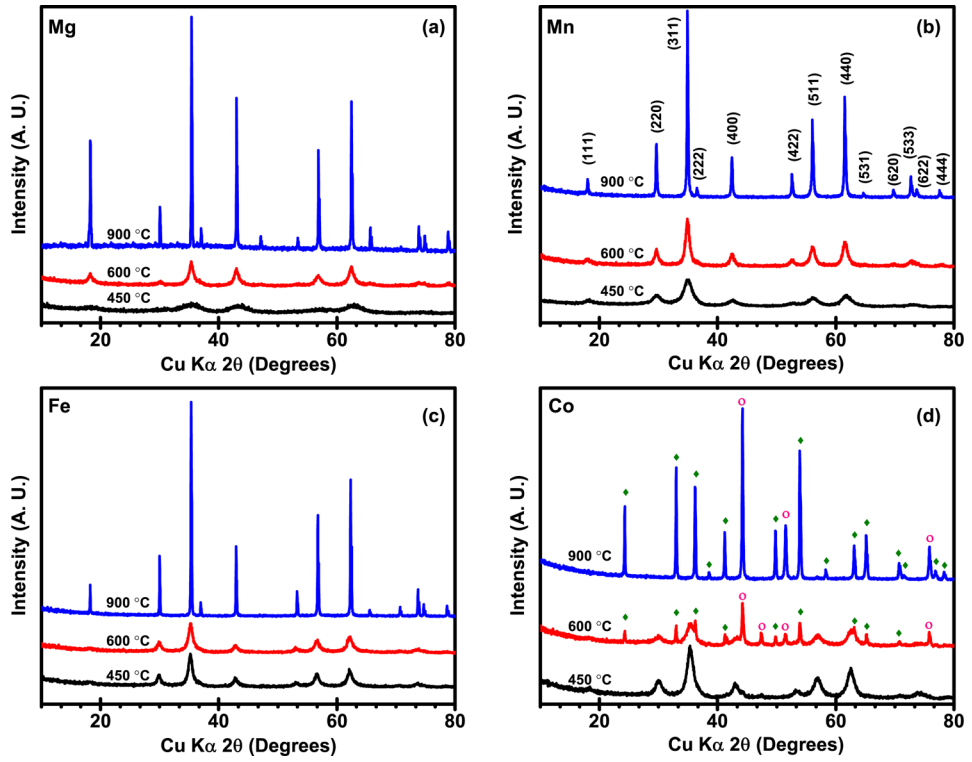

Figure 4. XRD patterns of (a) MgV_2O_4, (b) MnV_2O_4, (c) FeV_2O_4, and (d) CoV_2O_4 postheated to 450, 600, and 900 °C in 5% H_2−95% Ar for 12 h. The green diamond indicates V_2O_3 impurity, and pink circle indicates cobalt impurity.

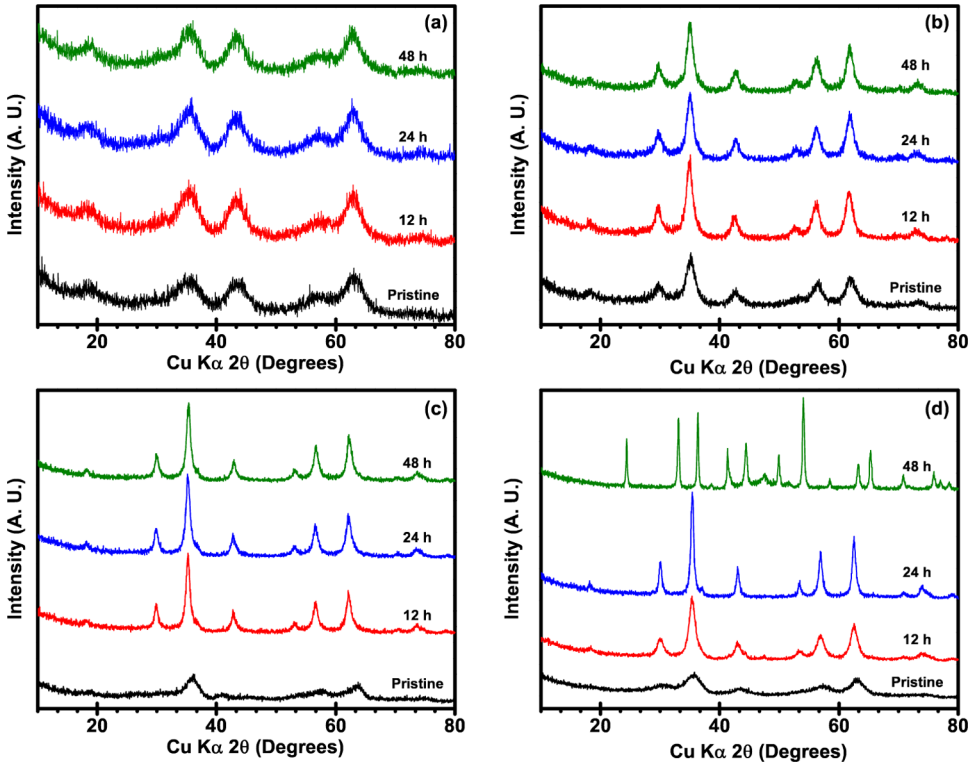

Figure 5. XRD patterns of (a) MgV_2O_4, (b) MnV_2O_4, (c) FeV_2O_4, and (d) CoV_2O_4 postheated to 450 °C in 5% H_2−95% Ar and held for 12, 24, and 48 h. The XRD pattern of the as-prepared samples is provided as a reference to the change in crystallinity after postheating.

Nevertheless, the primary particles appear to remain between 5 and 10 nm in diameter (see Supporting Information Figure S2b,d,f for a comparison) even when the dwell time was increased 8 times longer than the shortest dwell time (4 h vs 30 min). Several studies have demonstrated that microwave irradiation accelerates both the nucleation and crystal growth of materials,[26,27] but with a more pronounced effect on the nucleation stage. Our results provide further validation that

dx.doi.org/10.1021/ic5011506 | Inorg. Chem. 2014, 53, 8570−8576

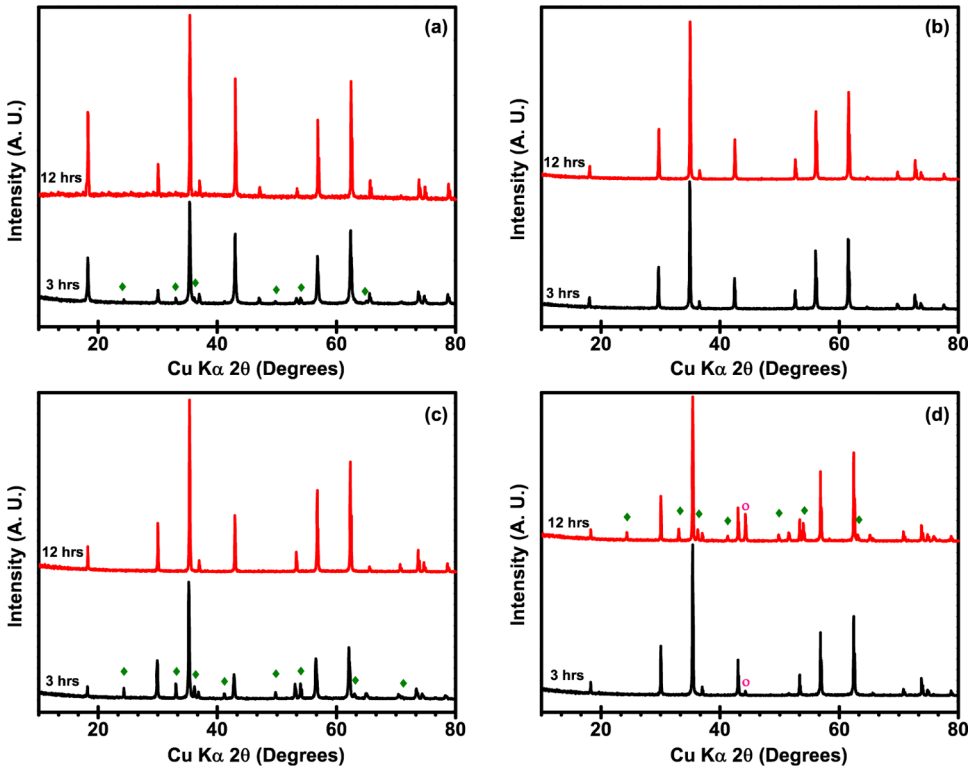

Figure 6. XRD patterns of (a) MgV_2O_4, (b) MnV_2O_4, (c) FeV_2O_4, and (d) CoV_2O_4 postheated to 900 °C in 100% Ar and held for 3 and 12 h. The green diamond in parts a and b indicates V_2O_3 impurity. The pink circle in part d indicates cobalt impurity.

microwave heating is more efficient in the nucleation stage compared to crystal growth as the primary particles do not vary significantly with changing dwell times (see Supporting Information Figure S2b,d,f for comparison), suggesting that the improvement in XRD sharpness is related to improved crystallinity to the small crystallites.

Postheat Treatment. Each of the AV_2O_4 samples (synthesized in the Monowave 300 reactor) was also subjected to postheat treatments to improve the crystallinity. The first treatment was carried out under 5% H_2−95% Ar atmosphere for 12 h at 450, 600, and 900 °C (Figure 4). As expected, the XRD peaks became sharper at higher temperatures. The MgV_2O_4 and MnV_2O_4 samples remained as pure phases even after heating at 900 °C. The FeV_2O_4 sample became pure phase with the postheating treatment at 450 °C and remained as pure phase up to 900 °C. The CoV_2O_4 sample began to disproportionate into Co metal and V_2O_3 at temperatures as low as 600 °C. By 900 °C, no spinel peaks were observed in the CoV_2O_4 (Figure 4d) sample. The as-prepared MgV_2O_4, MnV_2O_4, and FeV_2O_4 samples were also heated at 900 °C for 3 h under 5% H_2−95% Ar atmosphere. All XRD peaks (Figure S3 in Supporting Information) could be indexed to the spinel structure for MnV_2O_4, but the FeV_2O_4 and MgV_2O_4 samples had V_2O_3 impurity phase present with the shorter dwell time of 3 h at 900 °C.

Additional postheating treatments were carried out on AV_2O_4 (Mg, Mn, Fe, and Co) under 5% H_2−95% Ar atmosphere at 450 °C with hold times of 12, 24, and 48 h. The XRD peaks for AV_2O_4 (Mg, Mn, and Fe) did not increase in sharpness by extending the dwell time at 450 °C (Figure 5). In contrast, the sharpness of the XRD peaks for the CoV_2O_4 sample held for 24 h did improve as is evidenced by the ability to resolve the (222) peak (36.8°), which is hidden in the broadness of the (311) peak (~35°) in both the pristine sample and the sample held for 12 h at 450 °C. CoV_2O_4 breaks down into Co and V_2O_3 upon extending the dwell time to 48 h at 450 °C. The disproportionation of CoV_2O_4 under 5% H_2−95% Ar atmosphere at 900 °C, 12 h, and 450 °C, 48 h, suggests the environment is too reducing for Co^{2+} in CoV_2O_4.

In the interest of determining the effect of the atmosphere used in the postheating step, each of the AV_2O_4 samples was also heated at 900 °C and held for 3 and 12 h under Ar atmosphere (Figure 6). The MgV_2O_4 and FeV_2O_4 samples held for 3 h had V_2O_3 impurity phase present as seen in the XRD patterns (Figure 6a,c), suggesting that amorphous impurities may be present after the microwave process. The amount of impurity phase present in the Fe sample appears to be greater than that in the Mg sample (determined by the relative intensities of the peaks). With the loss of V from the FeV_2O_4 phase to form V_2O_3, the sample forms Fe_3O_4 spinel along with FeV_2O_4 spinel. A dwell time of 12 h was needed to obtain pure phase MgV_2O_4 and FeV_2O_4. In contrast, a pure phase MnV_2O_4 sample (Figure 6b) was obtained in as little as 3 h at 900 °C in Ar atmosphere. The MnV_2O_4 sample remained pure phase on extending the dwell time to 12 h.

The CoV_2O_4 phase was still present after heating to 900 °C (Figure 6d) in argon unlike the total disintegration of the spinel structure into Co and V_2O_3 under H_2−Ar atmosphere. Nevertheless, impurities were still present at both dwell times under argon atmosphere. The sample held for 3 h at the peak temperature had a small amount of Co impurity present. Upon extending the dwell time to 12 h, V_2O_3 precipitated out of the sample, and the amount of Co impurity increased. CoV_2O_4 was also heated to 700 and 800 °C under argon atmosphere for 3 h in an attempt to avoid the formation of cobalt metal impurity phase, but the impurity phase remained. The results confirm

dx.doi.org/10.1021/ic5011506 | Inorg. Chem. 2014, 53, 8570−8576

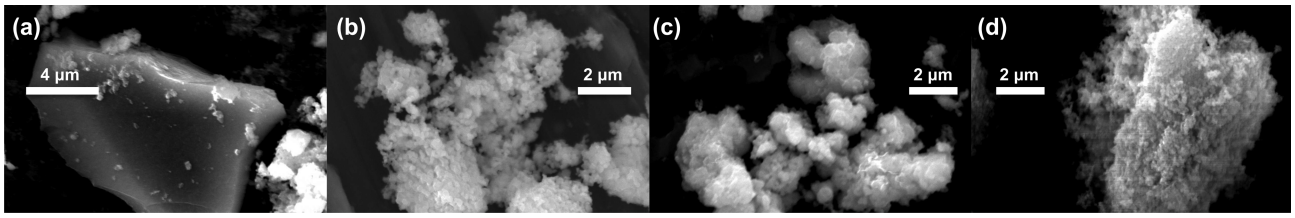

Figure 7. SEM images of (a) MgV_2O_4, (b) MnV_2O_4, (c) FeV_2O_4, and (d) CoV_2O_4 postheated to 900 °C for 12 h.

the difficulty of synthesizing CoV_2O_4 at high temperatures because of the ease with which Co^{2+} is reduced to Co metal. This demonstrates the importance of employing a low-temperature synthesis process for CoV_2O_4.

Figure 7 shows the morphology of each of the AV_2O_4 samples postheated to 900 °C. The Mn, Fe, and Co samples formed into secondary particles made up of the primary particles while the Mg sample formed very large primary particles. The differences in the morphology of the postheated samples may be caused by the differences in the melting temperature of the A^{2+} cations (Mg ~ 650 °C vs Fe, Mn, and Co >1200 °C).

CONCLUSIONS

We have demonstrated the use of a novel microwave-assisted solvothermal process for the synthesis of AV_2O_4 (Mg, Fe, Mn, and Co). This method is remarkably effective in reducing the synthesis time and energy use due to the efficiency of dielectric heating compared to conventional heating, which depends on convective currents and on the thermal conductivity of the constituents involved in the reaction. The ability to access V^{3+} is facilitated by the relative positions of the energy levels of the cations in solution, which are lower than those in the solid, combined with the use of a strong reducing solvent like TEG. The study also demonstrates that some spinel oxides like CoV_2O_4 are unstable at higher temperatures, so the MW-ST method presented here becomes valuable to access such metastable phases. The access to these spinel oxides by the MW-ST process provides an opportunity to tune systematically the V−V distance with solid solutions like $Co_{1-x}A_xV_2O_4$ (A = Mg, Mn, or Fe) with our future work and understand the role of V−V distance on localized to itinerant electron transition.

ASSOCIATED CONTENT

Supporting Information

Elemental ratios obtained from ICP analysis, XRD pattern for CoV_2O_4 synthesized in Monowave 300 and Synthos 3000 microwave reactor systems, SEM images of CoV_2O_4 synthesized in Synthos 3000 microwave reactor system and held for various times, and XRD patterns of AV_2O_4 (Mg, Mn, and Fe) postheated in argon atmosphere. This material is available free of charge via the Internet at http://pubs.acs.org.

AUTHOR INFORMATION

Corresponding Author

*E-mail: manth@austin.utexas.edu. Fax: +1 512-471-7681. Phone: +1 512-471-1791.

Author Contributions

Both A.G. and A.M contributed to the ideas and paper writing, and A.G. carried out the experiments.

Notes

The authors declare no competing financial interest.

ACKNOWLEDGMENTS

This work was supported by the office of Vehicle Technologies of the U.S. Department of Energy under Contract DE-AC0205CH11231 and the Welch Foundation Grant F-1254.

REFERENCES

(1) Manthiram, A.; Goodenough, J. B. *Can. J. Phys.* **1987**, *65*, 1309.
(2) Kato, Y.; Chern, G.-W.; Al-Hassanieh, K. A.; Perkins, N. B.; Batista, C. D. *Phys. Rev. Lett.* **2012**, *108*, 247215.
(3) Blanco-Canosa, S.; Rivadulla, F.; Pardo, V.; Baldomir, D.; Zhou, J. S.; García-Hernández, M.; López-Quintela, M.; Rivas, J.; Goodenough, J. *Phys. Rev. Lett.* **2007**, *99*, 187201.
(4) Pardo, V.; Blanco-Canosa, S.; Rivadulla, F.; Khomskii, D.; Baldomir, D.; Wu, H.; Rivas, J. *Phys. Rev. Lett.* **2008**, *101*, 256403.
(5) Baek, S. H.; Choi, K. Y.; Reyes, A. P.; Kuhns, P. L.; Curro, N. J.; Ramanchandran, V.; Dalal, N. S.; Zhou, H. D.; Wiebe, C. R. *J. Phys.: Condens. Matter* **2008**, *20*, 135218.
(6) Ebbinghaus, S. G.; Hanss, J.; Klemm, M.; Horn, S. *J. Alloys Compd.* **2004**, *370*, 75.
(7) Kismarahardja, A.; Brooks, J. S.; Zhou, H. D.; Choi, E. S.; Matsubayashi, K.; Uwatoko, Y. *Phys. Rev. B: Condens. Matter Mater. Phys.* **2013**, *87*, 054432.
(8) Huang, Y.; Yang, Z.; Zhang, Y. *J. Phys.: Condens. Matter* **2012**, *24*, 056003.
(9) Komarneni, S. *Curr. Sci.* **2003**, *85*, 1730.
(10) Polshettiwar, V.; Nadagouda, M. N.; Varma, R. S. *Aust. J. Chem.* **2009**, *62*, 16.
(11) Rao, K. J.; Vaidhyanathan, B.; Ganguli, M.; Ramakrishnan, P. A. *Chem. Mater.* **1999**, *11*, 882.
(12) Leonelli, C.; Lojkowski, W. *Chem. Today* **2007**, *25*, 34.
(13) Balaji, S.; Mutharasu, D.; Sankara Subramanian, N.; Ramanathan, K. *Ionics* **2009**, *15*, 765.
(14) Nethravathi, C.; Rajamathi, M. *Carbon* **2008**, *46*, 1994.
(15) Bilecka, I.; Niederberger, M. *Nanoscale* **2010**, *2*, 1358.
(16) Harrison, K. L.; Manthiram, A. *Chem. Mater.* **2013**, *25*, 1751.
(17) Muraliganth, T.; Murugan, A. V.; Manthiram, A. *J. Mater. Chem.* **2008**, *18*, 5661.
(18) Muraliganth, T.; Stroukoff, K. R.; Manthiram, A. *Chem. Mater.* **2010**, *22*, 5754.
(19) Vadivel Murugan, A.; Muraliganth, T.; Manthiram, A. *J. Electrochem. Soc.* **2009**, *156*, A79.
(20) Moorhead-Rosenberg, Z.; Harrison, K. L.; Turner, T.; Manthiram, A. *Inorg. Chem.* **2013**, *52*, 13087.
(21) Mizushima, K.; Jones, P. C.; Wiseman, P. J.; Goodenough, J. B. *Solid State Ionics* **1981**, *3*−*4*, 171.
(22) Baghbanzadeh, M.; Carbone, L.; Cozzoli, P. D.; Kappe, C. O. *Angew. Chem., Int. Ed.* **2011**, *50*, 11312.
(23) Liao, X.-H.; Zhu, J.-J.; Xu, J.-Z.; Chen, H.-Y.; Zhu, J.-M. *Chem. Commun. (Cambridge, U. K.)* **2001**, *2001*, 937.
(24) Liao, X.; Zhu, J.; Zhong, W.; Chen, H.-Y. *Mater. Lett.* **2001**, *50*, 341.
(25) Harrison, K. L.; Bridges, C. A.; Paranthanam, M. P.; Segre, C. U.; Katsoudas, J.; Maroni, V. A.; Idrobo, J. C.; Goodenough, J. B.; Manthiram, A. *Chem. Mater.* **2013**, *25*, 768.
(26) Jhung, S. H.; Jin, T.; Hwang, Y. K.; Chang, J. S. *Chem.—Eur. J.* **2007**, *13*, 4410.

(27) Serrano, D. P.; Uguina, M. A.; Sanz, R.; Castillo, E.; Rodríguez, A.; Sánchez, P. *Microporous Mesoporous Mater.* **2004**, *69*, 197.